

## Inherent Shear-Dilatation Coexistence in Metallic Glass \*

JIANG Min-Qiang(蒋敏强)<sup>1</sup>, JIANG Si-Yue(江思跃)<sup>1</sup>, DAI Lan-Hong(戴兰宏)<sup>1,2\*\*</sup>

<sup>1</sup>State Key Laboratory of Nonlinear Mechanics, Institute of Mechanics, Chinese Academy of Sciences, Beijing 100190

<sup>2</sup>State Key Laboratory of Explosion Science and Technology, Beijing Institute of Technology, Beijing 100081

(Received 3 October 2008)

*Shear deformation can induce normal stress or hydrostatic stress in metallic glasses [Nature Mater. 2 (2003) 449, Intermetallics 14 (2006) 1033]. We perform the bulk deformation of three-dimensional Cu<sub>46</sub>Zr<sub>54</sub> metallic glass (MG) and Cu single crystal model systems using molecular dynamics simulation. The results indicate that hydrostatic stress can incur shear stress in MG, but not in crystal. The resultant pronounced asymmetry between tension and compression originates from this inherent shear-dilatation coexistence in MG.*

PACS: 61.43.Dq, 62.20.De, 64.70.Pe, 81.05.Kf

Metallic glasses (MGs) display many different mechanical properties compared with crystalline cousins, because of their disordered atomic structure.<sup>[1,2]</sup> For example, magnitudes of yield stresses in compression are usually greater than those in tension, exhibiting a strength-differential (SD) effect.<sup>[3,4]</sup> Meanwhile, the fracture angles always deviate from 45°, i.e. the maximum shear stress direction,<sup>[3–5]</sup> implying pressure or normal stress sensitivity. The deviation is also tension-compression asymmetric.<sup>[3–5]</sup> Furthermore, it has been widely found that imposed high pressure will induce structural change<sup>[6–8]</sup> and enhance ductility of MGs.<sup>[9]</sup> The pressure-sensitivity of mechanical behaviour has attracted substantial interest,<sup>[10–12]</sup> since it is critical to engineering applications of MGs. The underlying mechanism is believed to be contributed to the shear-induced dilatation of randomly close-packed atoms within MGs.<sup>[13]</sup> This physical picture must cover two opposite, but coexistent aspects.<sup>[4]</sup> On the one hand, shear deformation induces volume changing or hydrostatic stress. On the other hand, the volume/bulk deformation should also produce shear stress. The former has been confirmed by a series of experiments and molecular dynamics (MD) simulations.<sup>[11,14,15]</sup> However, there is no work in respect of the latter up to now. Since the bulk moduli of MGs are often large,<sup>[13]</sup> a little change in volume needs very great hydrostatic stress. In addition, a pure bulk loading without inducing any shear deformation is also very difficult for a real experiment. Note that Knuyt *et al.* has successfully simulated the bulk deformation of an amorphous metal to calculate its elastic constants by using MD method.<sup>[16]</sup> In this Letter, we rely on MD computer simulations on a Cu<sub>46</sub>Zr<sub>54</sub> MG to investigate whether the pure bulk deformation can induce shear stress or not. For comparison, the bulk deformation of a Cu single crystal is also performed,

the simulation details and other results will be presented elsewhere.

In our MD simulations, we take a three-dimensional binary MG system in which Cu<sub>46</sub>Zr<sub>54</sub> containing 27436 atoms is used. Atoms interact via a modified Lennard-Jones 4–8 potential in the form:<sup>[17]</sup>

$$\phi_{ij}(r_{ij}) = \begin{cases} -\frac{A}{r_{ij}^4} + \frac{B}{r_{ij}^8} + Cr_{ij} + D, & \text{for } 0 < r_{ij} \leq r_t, \\ 0, & \text{for } r_{ij} > r_t, \end{cases} \quad (1)$$

where  $r_{ij}$  is the distance between the atoms  $i$  and  $j$ ;  $A$ ,  $B$ ,  $C$  and  $D$  are constants whose values are available in Ref. [17];  $r_t$  is the truncation distance with the values of 5.08, 5.58 and 6.00 Å for Cu–Cu, Cu–Zr and Zr–Zr pairs, respectively. The motion of each atom was evaluated by integrating the Newtonian equations of motion using the velocity-Verlet method with a time step of 1 fs. To form an amorphous structure, the melt-quench procedure was used. We start the procedure by building an initial structure and set the initial conditions. The initial structure was created by placing all atoms into an *fcc* crystal lattice in a random order; the initial conditions were applied by using periodic boundary conditions (PBC) in all three dimensions and setting the initial velocities of all atoms to zero. After that, we gradually heated the structure to 2400 K for sufficiently melting, then cooled it down to 300 K with the cooling rate of 10 K/ps. The global stress tensor of the as-built structure was calculated based on Eq. (1) using<sup>[18]</sup>

$$\sigma_{ab} = \frac{1}{V} \left( - \sum_i m_i v_i^a v_i^b + \frac{1}{2} \sum_i \sum_{j \neq i} \frac{\partial \phi_{ij}(r_{ij})}{\partial r_{ij}} \frac{r_{ij}^a r_{ij}^b}{r_{ij}} \right), \quad (2)$$

\*Supported by the National Natural Science Foundation of China under Grant Nos 10725211, 10721202 and 10872206, and the Key Project of Chinese Academy of Sciences under Grant Nos KJCX-SW-L08 and KJCX2-YW-M04.

\*\*To whom correspondence should be addressed. Email: lhdai@lnm.imech.ac.cn

© 2009 Chinese Physical Society and IOP Publishing Ltd

where  $V$  is the volume of the computational cell;  $r_{ij}^a$  and  $r_{ij}^b$  represent the separation distances between atoms  $i$  and  $j$  along any two given principle directions  $a$  and  $b$ , respectively;  $m_i$  is the mass of atom  $i$ ;  $v_i^a$  and  $v_i^b$  denote the velocity components of atom  $i$  along the directions  $a$  and  $b$ , respectively. To allow the initial glassy structure to find a local energy minimum with near-zero stress components, we repeatedly adjusted their dimensions, and reposition each atom accordingly. Finally, an MG sample I with the size of  $80 \times 80 \times 80 \text{ \AA}^3$  is guided toward a low-stress state (the normal stress components were kept at zero and the shear stress components were maintained below 10 MPa). A 32000-atoms Cu single crystal sample II with the size of  $72 \times 72 \times 72 \text{ \AA}^3$  was also created for comparison. The radial distribution functions (RDF) of the two samples were examined and displayed in Figs. 1(a) and 1(b), respectively. The RDF figures confirm the perfect amorphous structure for sample I and crystal feature for sample II.<sup>[19]</sup>

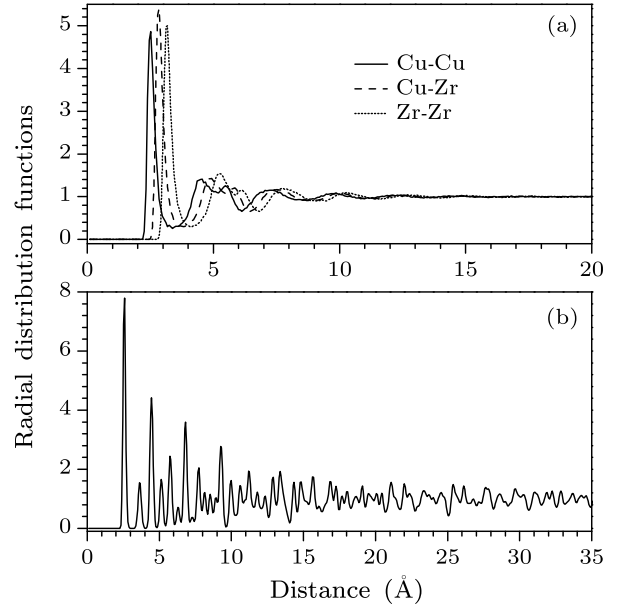


**Fig. 1.** Radial distribution functions for (a)  $\text{Cu}_{46}\text{Zr}_{54}$  metallic glass sample and (b) Cu single crystal.

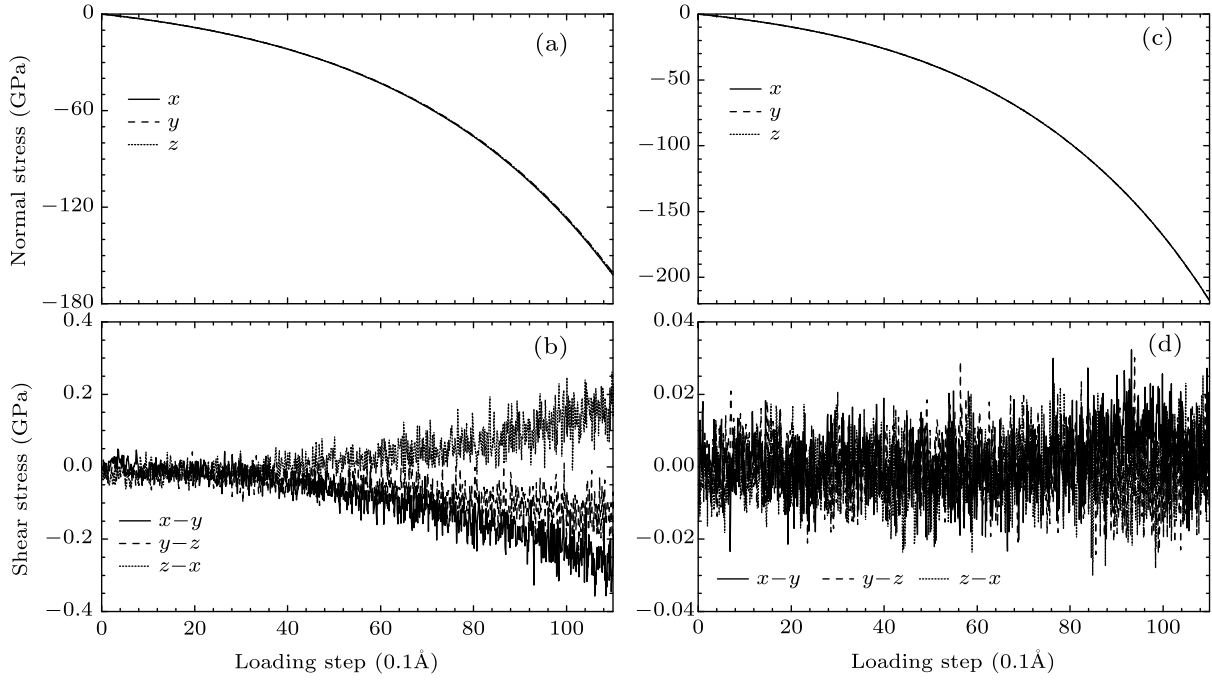


**Fig. 2.** Stress-loading displacement curves: (a) normal stresses and (b) shear stresses of  $\text{Cu}_{46}\text{Zr}_{54}$  metallic glass; (c) normal stresses and (d) shear stresses of Cu single crystal.

To explore the bulk deformation behaviour of MG sample, we gradually reduced the size of the computational cell in all three dimensions at a constant rate. The lengths of the cells decrease  $0.1 \text{ \AA}$  per step, and the boundaries were held on for 3 ps for relaxation. In the loading procedure, PBC was still used on all the boundaries, and the temperature of the sample was kept at 300 K. Finally, total 110 load steps were applied, ensuring that the total potential energy is not greater than zero. Figure 2 shows the evolution of the six stress components during loading, where the Cu single crystal case is also presented on the right

hand. From this picture, it can be clearly seen that for MG sample (see Figs. 2(a) and 2(b)), the hydrostatic stress ( $\sigma_{xx} \approx \sigma_{yy} \approx \sigma_{zz}$ ), if it is large enough, can induce gradual increasing in shear stress. However, for Cu single crystal sample (see Figs. 2(c) and 2(d)), the three shear stress components always keep constant, i.e. the initial value of zero, under almost the same hydrostatic stresses. This difference between them should be contributed to their distinct atomic structures. Crystals can deform without changing shape because the periodicity along the loading directions provides a uniform compression or tension. A bulk

deformed portion of an MG material, on the other hand, does not find a perfect fit; the shear motions among disordered atoms must take place. Recently, the nanoscale dimples and periodic corrugations have been widely observed on the dynamic mode I fracture planes of MGs.<sup>[4,20–22]</sup> In such a case, the underlying fracture mechanism is the quasi-cleavage via tension transformation zones (TTZs), during which the broken of atomic clusters by tension can bring out the shear motion/flow within the cluster.<sup>[4]</sup> These nanoscale patterns are considered as the indicative of shear flow at atomic level induced by normal tension stress.<sup>[4,20,22]</sup> Our simulation result provides an evidence for energy dissipation underpinning these brand-new fracture patterns.

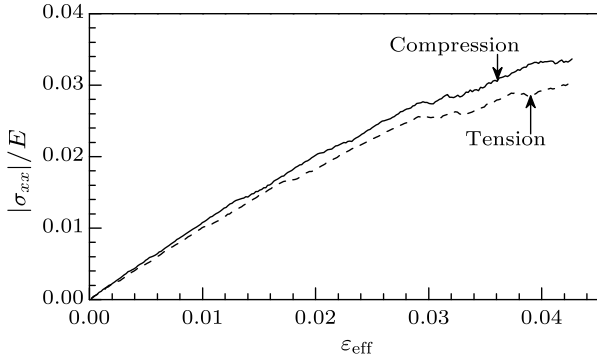


**Fig. 3.** Results of two uniaxial straining simulations using the same initial structure, one in compression and the other in tension.

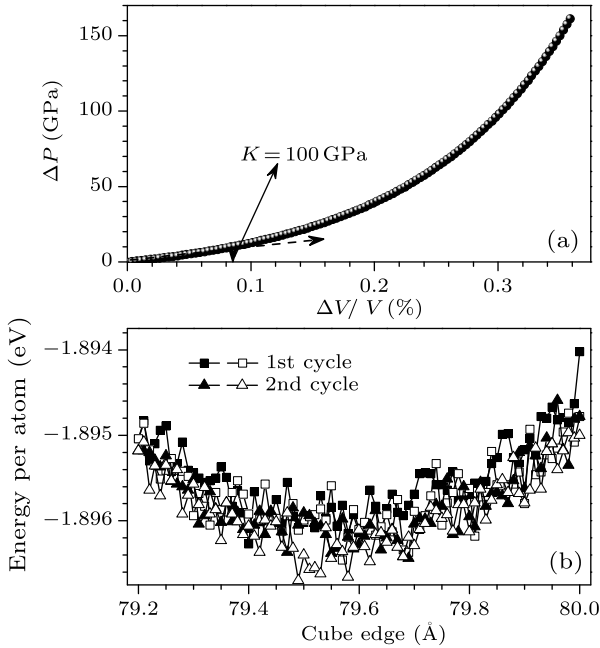


**Fig. 4.** (a) Dependence of hydrostatic stress increment on volume change, where the initial slope is calculated to be about 100 GP. (b) Two cycles for the atomic energy as a function of the cube edge.

Based on our present simulations and previous works,<sup>[4,11,13–15]</sup> one can conclude that the shear and

bulk deformations are coexistent inherently in metallic glasses. This characteristic determines most behaviour of deformation and failure of MGs,<sup>[3–5,20–24]</sup> such as toughness, ductility, fracture patterning, yield strength and so on. In order to recover this point, we performed typical uniaxial tension and compression simulations on the same MG sample, respectively. Figure 3 shows the relationship between the stress normalized by Young's Modulus of 65 GPa and the equivalent strain. It is noted that there is indeed an obvious asymmetry in the plastic mechanical response: the yield strength in compression is higher than that in tension, which has been widely observed in many real experiments.<sup>[4,5]</sup> The difference of the yield strength in the value is about 8%, which can be measured by the method described in Ref. [17].

Finally, this bulk deformation method in our present work provides a useful tool to calculate the bulk modulus  $K$ . The usual expression for  $K$  is given by

$$K = -\frac{\partial P}{\partial V/V}, \quad (3)$$

where  $P = (\sigma_{xx} + \sigma_{yy} + \sigma_{zz})/3$  indicates the pressure of a sample, and  $V$  denotes the volume of the sample. The pressure increment (i.e.  $\partial P$ ) varies with the relative change of the volume (i.e.  $\partial V/V$ ) for the MG sample, as displayed in Fig. 4(a). Thus, the initial slope of the curve represents its initial bulk modulus. After calculation, we find that initial bulk modulus of the metallic glass sample is about 100 GPa, which is very close to the value tested by experimental method.<sup>[25]</sup> From Eq. (3), the alternative expression for  $K$  can be derived as<sup>[16]</sup>

$$K = \frac{N_{\text{at}}}{9l_{\text{min}}} \left( \frac{d^2 E_{\text{at}}}{dl^2} \right) \Big|_{l_{\text{min}}}, \quad (4)$$

where  $N_{\text{at}}$  is the number of atoms,  $E_{\text{at}}$  the mean atomic energy, and  $l_{\text{min}}$  the edge length  $l$  for which the total energy is minimum. In practice,  $K$  is calculated with the following process. We started from an atomic configuration very near to the minimum-energy situation (the initial configuration can be satisfied). Then,  $l$  was decreased in eighty steps of 0.01 Å; next  $l$  was increased in the same number of steps until the starting value was reached. In this way, a small cycle of  $l$  values was realized. Two cycles were performed, as shown in Fig. 4(b). For each step in the cycle, all atoms were allowed to relax to the minimum energy.  $E_{\text{at}}$  for a certain  $l$  value was taken as the average between the four values calculated the two cycles. The  $E_{\text{at}}(l)$  dependence was then approximated by a parabola from its parameters accurate values of  $l_{\text{min}}$  and  $d^2 E_{\text{at}}/dl^2$  were determined, so that the bulk modulus was calculated to be 0.655 eV·Å<sup>3</sup> using Eq. (4). This value corresponds to about 105GP, which agrees well with that calculated by Eq. (3). The good agreement between

our simulations and experimental measurements, in turn, implies that the present bulk loading procedure is technically correct and the simulation results are believable.

In summary, we have performed MD simulations of a 3D model Cu–Zr metallic glass to investigate the shear deformation under bulk loading conditions. The results clearly show that the bulk deformation can give rise to the increasing in shear stresses in MGs. However, this phenomenon is not observed in crystal sample. This coexistent shear-bulk deformation can be considered as an inherent property of metallic glasses, which is responsible for the resultant tension-compression asymmetry in the plastic mechanical response. The calculated bulk modulus using the present bulk loading is shown to compare favourably with the experimental data, which in turn validates our simulations.

## References

- [1] Bernal J D 1960 *Nature* **185** 68
- [2] Sheng H W et al 2006 *Nature* **439** 419
- [3] Zhang Z F et al 2003 *Acta Mater.* **51** 1167
- [4] Jiang M Q et al 2008 *Phil. Mag.* **88** 407
- [5] Zhang Z F et al 2003 *Phys. Rev. Lett.* **91** 045505
- [6] Wang W H et al 2000 *Phys. Rev. B* **61** 3166
- [7] Jiang J Z et al 2002 *Appl. Phys. Lett.* **81** 4347
- [8] Li G et al 2007 *Chin. Phys. Lett.* **24** 2323
- [9] Yu P et al 2007 *Appl. Phys. Lett.* **90** 051906
- [10] Flores et al 2001 *Acta Mater.* **49** 2527
- [11] Schuh et al 2003 *Nature Mater.* **2** 449
- [12] Ai K et al 2007 *Scripta Mater.* **56** 761
- [13] Jiang M Q et al 2007 *Phys. Rev. B* **76** 054204
- [14] Li J et al 2002 *Phil. Mag.* **82** 2623
- [15] Ogata et al 2006 *Intermetallics* **14** 1033
- [16] Knuyt G et al 1986 *J. Phys. F: Met. Phys.* **16** 1989
- [17] Lund A C et al 2003 *Acta Mater.* **51** 5399
- [18] Born M et al 1954 *Dynamical theory of crystal lattices* (Oxford: Clarendon)
- [19] Andrew R L 1996 *Molecular Modeling: Principles and Applications* (London: Addison-Wesley Longman)
- [20] Xi X K et al 2005 *Phys. Rev. Lett.* **94** 125510
- [21] Shen J et al 2006 *Appl. Phys. Lett.* **89** 121908
- [22] Wang G et al 2007 *Phys. Rev. Lett.* **98** 235501
- [23] Dai L H 2004 *Chin. Phys. Lett.* **21** 1593
- [24] Liu L F 2008 *Chin. Phys. Lett.* **25** 1052
- [25] Wang W H 2006 *J. Appl. Phys.* **99** 1